Romanian Reports in Physics, Vol. 59, No. 4, P. 987–1002, 2007

Dedicated to Prof. Dumitru Barbu Ion's 70th Anniversary

STANDARD MODEL HIGGS PHYSICS AT COLLIDERS

A. ROSCA

West University of Timişoara, Faculty of Physics, Bd. Vasile Parvan 4, RO-300223 Timişoara, Romania; e-mail: rosca@physics.uvt.ro

(Received August 8, 2007)

Abstract. In this report we briefly review the experimental status and prospects to verify the Higgs mechanism of spontaneous symmetry breaking. The focus is on the most relevant aspects of the phenomenology of the Standard Model Higgs boson at current (Tevatron) and future (Large Hadron Collider, LHC and International Linear Collider, ILC) particle colliders. We review the Standard Model searches: searches at the Tevatron, the program planned at the LHC and prospects at the ILC. Emphasis is put on what follows after a candidate discovery at the LHC: the various measurements which are necessary to precisely determine what the properties of this Higgs candidate are.

Key words: spontaneous symmetry breaking, Higgs boson, collider.

1. INTRODUCTION

One of the most important open questions of contemporary particle physics is the origin of the electroweak symmetry breaking. In 1964 the Higgs mechanism was proposed by Higgs, Kibbe, Guralnik, Hagen, Englert and Brout [1] which has become part of the Standard Model (SM) of particle physics. A large theoretical and experimental effort has been devoted to the study of the scalar Higgs boson predicted by the Higgs mechanism in the SM. The discovery of this particle is among the most important goals of both the Tevatron and the Large Hadron Collider, while the precise determination of its physical properties strongly supports the need for a future e^+e^- Linear Collider.

The Tevatron at Fermilab collides protons and antiprotons at a center-of-mass energy of 1.96 TeV. The machine has delivered over 1 fb^{-1} of data to the two experiments, CDF and DØ. The improved detectors, higher center-of-mass energy and the increase in luminosity enable the experiments to significantly extend previous searches and provide them with a substantial discovery potential.

The Large Hadron Collider at CERN and the International Linear Collider are machines under construction and in the planning phase. The LHC will collide protons with protons at a center-of-mass energy of 14 TeV. First collisions are expected in 2008. The two experiments, ATLAS and CMS, have made detailed

studies on their potential to explore the Higgs mechanism and to discover new physics. The ILC will collide electrons and positrons with a center-of-mass energy of several hundred GeV. It will be the next generation machine for precision measurements of electroweak parameters improving the results of its predecessor, the Large Electron Positron (LEP) collider.

2. THE HIGGS MECHANISM

In Yang-Mills theories gauge invariance forbids in the Lagrangian an explicit mass term for the gauge bosons. While this is acceptable for theories like Quantum Electrodynamics (QED) and Quantum Chromodynamics (QCD) where both photon and gluons are massless, it is unacceptable for the gauge theory of weak interactions, since both the charged $W^{\pm}$ and neutral Z^0 gauge bosons have large masses ($M_W \simeq 80$ GeV, $M_Z \simeq 91$ GeV). A possible solution to this problem was proposed by several physicists in 1964 [1] and it is known today as the Higgs mechanism.

The Standard Model is a spontaneously broken Yang-Mills theory based on the $SU(2)_L \times U(1)_Y$ non-abelian symmetry group [2]. The Higgs mechanism is implemented in the SM by introducing a weak isospin doublet of complex scalar fields ϕ with hypercharge $Y_\phi = 1/2$,

$$\phi = \begin{pmatrix} \phi^+ \\ \phi^0 \end{pmatrix}. \tag{1}$$

The Lagrangian reads

$$\mathcal{L}_\phi = (D^\mu \phi)^\dagger D_\mu \phi - \mu^2 \phi^\dagger \phi - \lambda (\phi^\dagger \phi)^2, \tag{2}$$

where $D^\mu \phi = (\partial_\mu - igW_\mu^a \tau^a - ig' Y_\phi B_\mu)$ and $\tau^{-a} = \sigma^a/2$ for $a = 1, 2, 3$ are the $SU(2)$ Lie Algebra generators, proportional to the Pauli matrix σ^a. The gauge symmetry of the Lagrangian is broken to the $U(1)_{em}$ when a particular vacuum expectation value is chosen, for instance:

$$\langle \phi \rangle = \frac{1}{\sqrt{2}} \begin{pmatrix} 0 \\ v \end{pmatrix} \qquad \text{with} \qquad v = \left(\frac{-\mu^2}{\lambda} \right)^{1/2} \qquad (\mu^2 < 0,\ \lambda > 0). \tag{3}$$

Upon spontaneous symmetry breaking the kinetic term in equation (2) gives rise to the SM gauge boson mass terms. We will obtain the mass terms for the charged gauge bosons $W_\mu^\pm$:

$$W_\mu^\pm = \frac{1}{\sqrt{s}} (W_\mu^1 \pm W_\mu^2) \rightarrow M_W = g \frac{v}{2}, \tag{4}$$

and for the neutral gauge boson Z_μ^0 :

$$Z_\mu^0 = \frac{1}{\sqrt{g^2+g'^2}}(gW_\mu^3 - g'B_\mu) \longrightarrow M_Z = \sqrt{g^2+g'^2}\,\frac{v}{2}, \tag{5}$$

while the orthogonal linear combination of W_μ^3 and B_μ remains massless and corresponds to the photon field (A_μ):

$$A_\mu = \frac{1}{\sqrt{g^2+g'^2}}(g'W_\mu^3 + gB_\mu) \longrightarrow M_A = 0, \tag{6}$$

the gauge boson of the residual $U(1)_{em}$ gauge symmetry.

The content of the scalar sector of the theory becomes more transparent if one works in the unitary gauge and eliminates the unphysical degrees of freedom using gauge invariance. After parameterizing and rotating the $\phi(x)$ complex scalar field as follows:

$$\phi(x) = \frac{e^{\frac{i}{v}\chi(x)\cdot\vec{\tau}}}{\sqrt{2}}\begin{pmatrix}0\\ v+H(x)\end{pmatrix} \xrightarrow{SU(2)} \phi(x) = \frac{1}{\sqrt{2}}\begin{pmatrix}0\\ v+H(x)\end{pmatrix}, \tag{7}$$

the scalar potential in equation (2) becomes:

$$\mathcal{L}_\phi = \mu^2 H^2 - \lambda v H^3 - \frac{1}{4}H^4 = -\frac{1}{2}M_H^2 H^2 - \sqrt{\frac{\lambda}{2}}M_H H^3 - \frac{1}{4}\lambda H^4. \tag{8}$$

Three degrees of freedom, the $\chi^a(x)$ Goldstone bosons, have been reabsorbed into the longitudinal components of the $W_\mu^\pm$ and Z_μ^0 weak gauge bosons. One real scalar field remains, the Higgs boson H, with mass $M_H^2 = -2\lambda^2 = 2\lambda v^2$.

The couplings of the Higgs boson to the gauge fields are proportional to their mass. Therefore H does not couple to the photon at tree level. Decays into final states not allowed at tree level proceed via loop diagrams. Particularly relevant to the SM Higgs boson phenomenology are the decays of the Higgs boson to pairs of photons, and to a photon and a Z_μ^0 weak boson, as well as the decays to a pair of gluons.

The Standard Model gauge symmetry also forbids explicit mass terms for the fermionic degrees of freedom of the Lagrangian. The fermion mass terms are then generated via gauge invariant Yukawa couplings to the scalar field ϕ:

$$\mathcal{L}_{Yukawa} = -y_u \bar{Q}_L \phi^c u_R - y_d \bar{Q}_L \phi d_R - y_\ell \bar{L}_L \phi \ell_R + h.c. \tag{9}$$

where $\phi^c = -i\sigma^2\phi^*$ and y_f $(f = u, d, \ell)$ are the Yukawa couplings, arbitrarily introduced to realize the coupling between the ϕ and the fermionic fields of the

SM. Q_L and L_L represent the quark and lepton left handed doublets of $SU(2)_L$, while u_R, d_R, and ℓ_R are the corresponding right handed singlets. Since the scalar fields ϕ has a non zero vacuum expectation value through spontaneous symmetry breaking, each fermion degree of freedom coupled to a field ϕ develops a mass term with mass parameter $M_f = y_f \frac{v}{\sqrt{2}}$. The Yukawa coupling of the f fermion to the Higgs boson, y_f, represents a free parameter of the SM Lagrangian.

3. PHENOMENOLOGY OF THE HIGGS BOSON

At the tree level, the SM Higgs boson can decay into pairs of electroweak gauge bosons, $H \to W^+W^-$, ZZ and into pairs of quarks and leptons, $H \to q\bar{q}$, $\ell^+\ell^-$. At one-loop it can decay into two photons, $H \to \gamma\gamma$, or a γZ pair, $H \to \gamma Z$. Fig. 1 (left) shows all the decay branching ratios of the SM Higgs boson as functions of its mass M_H, including all available QCD and electroweak radiative corrections, calculated with HDECAY [3]. The Higgs boson total width, sum of all the partial widths $\Gamma(H \to XX)$, is represented in Fig. 1 (right). One can see from Fig. 1 (left) that a light Higgs boson, $M_H \leq 130$–140 GeV, behaves very differently from a heavy Higgs boson, $M_H \geq 130$–140 GeV. A light Higgs boson mainly decays into a $b\bar{b}$ pair, followed by all other pairs of lighter fermions. Loop-induced decays also play a role in this region. $H \to gg$ is dominant among them and can be larger than many tree level decays. Unfortunately, this decay mode is rather unusable, in particular at hadron colliders, because of large backgrounds from QCD processes. Among radiative decays, the decay $H \to \gamma\gamma$ is very small, but it is actually very important because the mass peak can be seen in

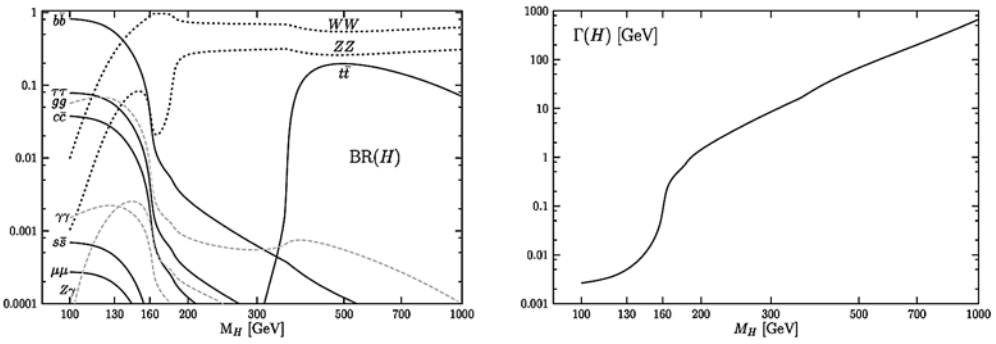

Fig. 1 – SM Higgs decay branching ratios as a function of M_H [4] (left) and the total decay width [4] (right).

the two-photon invariant mass spectrum on top of a large background using an excellent electromagnetic calorimeter. On the other hand, for larger Higgs masses, the decays to W^+W^- and ZZ dominate. All decays into fermions or loop-induced decays are suppressed, except $H \to t\bar{t}$ for Higgs masses above the $t\bar{t}$ production threshold. There is an intermediate region, around $M_H \simeq 160$ GeV, below the W^+W^- and ZZ thresholds, where the decays into WW^* and ZZ^* become important, with one of the two gauge bosons being off-shell. These are three-body decays of the Higgs boson that start to dominate over the $H \to b\bar{b}$ two-body decay mode when the relatively large HWW or HZZ couplings compensate for their phase space suppression.

3.1. EXPERIMENTAL SEARCHES

The current lower limit on the Higgs mass of 114.4 GeV at 95% confidence level (C.L.) comes from the LEP experiments [5]. The LEP experiments pushed the lower limit on the Higgs boson mass well above the Z pole. In this mass range it would be difficult to detect it at proton-antiproton machines. The Tevatron is the current place for Higgs searches which is sensitive to Higgs boson masses around 130 GeV.

The processes through which a SM Higgs boson can be produced at the Tevatron and the LHC are illustrated in Figs. 2 and 3. The cross sections for all these production modes as functions of M_H are summarized in Fig. 4 and contain all known orders of QCD corrections.

The major production mode is gluon-gluon fusion, $gg \to H$, a loop induced process, greatly enhanced by the top-quark contribution. For light and intermediate mass Higgs bosons, the large cross section of this process must compensate the large hadronic background. In this mass range, the Higgs boson mainly decays into $b\bar{b}$ pairs and therefore there is no other non-hadronic probe that can help distinguishing this final state from the overall hadronic activity in the detector. To reduce the background, one has often to employ rare Higgs decay modes, like $H \to \gamma\gamma$. For larger Higgs masses, above the ZZ threshold, gluon-gluon fusion together with $H \to ZZ$ produces a very distinctive signal and makes this a very

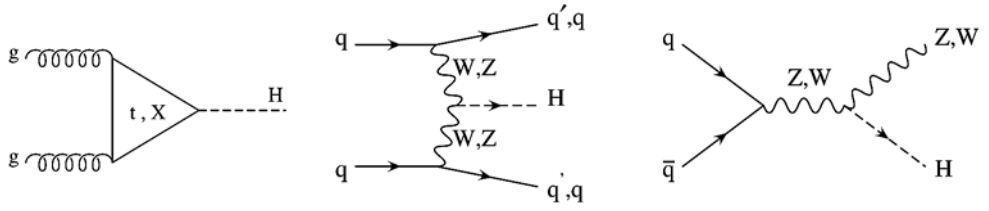

Fig. 2 – Main Higgs production processes at hadron colliders: $gg \to H$, $qq \to qqH$, and $q\bar{q} \to WH, ZH$.

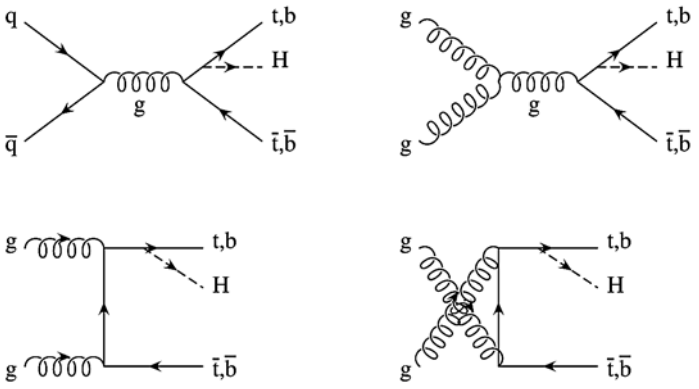

Fig. 3 – Higgs boson production in association with heavy quarks.

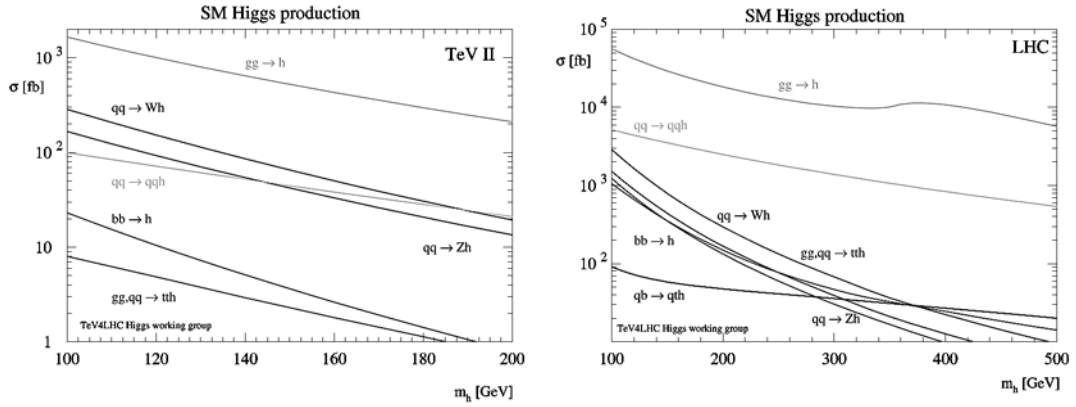

Fig. 4 – Cross sections for Higgs boson production processes at the Tevatron, Run II ($\sqrt{s}$=1.96 TeV) [6] (left) and at the LHC ($\sqrt{s}$=14 TeV) [6] (right).

important channel for detection. For this reason, $gg \to H$ plays a fundamental role at the LHC over the entire boson mass range, but is of very limited use at the Tevatron, where it can only be considered for Higgs masses very close to the upper reach of the accelerator.

Weak boson fusion ($qq \to qqH$, see second diagram in Fig. 2) and the associated production with weak gauge bosons ($q\bar{q} \to WH$, ZH, see third diagram in Fig. 2) have rather large cross sections, of different relative size at the Tevatron and at the LHC. The reaction $q\bar{q} \to WH$, ZH is particularly important at the Tevatron, where only a relative light Higgs boson will be accessible.

The production of a SM Higgs boson with heavy quarks, in the two channels $q\bar{q}$, $gg \to q\bar{q}H$, with $q = t, b$, see Fig. 3, is small at both Tevatron and the LHC, but has a great physics potential. The associated production with $t\bar{t}$ pairs is

probably too small to be seen at the Tevatron, given the expected luminosities, but will play a very important role for a light SM Higgs boson at the LHC, where enough statistics will be available to fully exploit the signature of a $t\bar{t}H$, $H \to b\bar{b}$ final state. Moreover, at the LHC, the associated production of a Higgs boson with top quarks will offer a direct handle on the top-quark Yukawa coupling. The production of a SM Higgs boson with $b\bar{b}$ pairs is very small, since the SM bottom-quark Yukawa coupling is suppressed by the bottom quark mass. This makes the $b\bar{b}H$, $H \to b\bar{b}$ channel an ideal candidate to provide evidence of new physics.

3.1.1. Higgs searches at Tevatron

We briefly discuss further the main Higgs boson search channels at Tevatron. The preliminary results of the two experimental collaborations are accessible through their web pages [7].

1. $\mathbf{ZH \to \nu\bar{\nu}b\bar{b}}$

This channel is very sensitive because of the large branching ratios for the $Z \to \nu\bar{\nu}$ and $H \to b\bar{b}$ decays. The signature for the final state are two acoplanar jets with a transverse momentum above 60 and 25 GeV, of which at least one has to be b-tagged. To account for the two neutrinos which leave the collision undetected a missing transverse energy above 70 GeV is required in the analysis. Main background sources are W/Z production associated with heavy flavor jets, multi-jet production, di-boson production, mis-tagged b-jets and $t\bar{t}$ pair production. For a Higgs mass of 120 GeV and using 289 pb^{-1} of integrated luminosity CDF observes six events while 4.36 ± 1.02 events are predicted. This leads to a 95% C.L. exclusion limit of 4.5 pb. Including 261 pb^{-1} of data DØ observes 11 events and 9.4 ± 1.8 are predicted, leading to an exclusion limit of 4.3 pb at 95% C.L. Using this analysis, limits on WH production with a missed charged lepton can be deduced. This improves the combined limits on WH production.

2. $\mathbf{WH \to \ell\nu b\bar{b}}$

This final state consists of two b jets from the Higgs boson and a charged lepton, electron or muon, together with a neutrino from the decay of the W boson. CDF selects events with jets having a transverse momentum above 15 GeV, the electron or muon above 20 GeV transverse momentum and the missing transverse energy higher than 20 GeV. The analysis is done separately for single and double b-tagged events. Based on an integrated luminosity of 695 pb^{-1}, 332 events with at least one b-tagged jet are observed. The background consists of mis-tagged events, $Wb\bar{b}$, $Wc\bar{c}$, Wc, $t\bar{t}$, single top, di-boson and multi-jet production. The prediction of total background amounts to 318.8 ± 54.7 events. Limits are derived by fitting

the di-jet invariant mass spectrum. For a Higgs mass of 115 GeV an upper exclusion limit of 3.6 pb at 95% C.L. has been established.

DØ does the WH analyses separately in the electron and the muon channel, plus the missed lepton channel as mentioned above in the ZH analysis. The limit is derived from counting the number of events inside an invariant jet-jet mass window around a Higgs mass of 115 GeV. The integrated luminosity used varies slightly for the different WH search channels and ranges from 371 to 385 pb^{-1}. 32 single b-tagged events and six double b-tagged events are observed. The number of predicted events amounts to 45.1 ± 6.9 and 9.3 ± 1.8. A combined exclusion limit of 2.5 pb at 95% C.L. can been established.

3. $\mathbf{WH \to WWW^* \to \ell^\pm\ell^\pm + X}$

The WH production with three W bosons (of which at least two are on-shell) is considered in the final state with two like-sign leptons, i.e. one lepton from the Higgs and one lepton from the associated W boson. In this way the background of Z bosons decaying into a pair of charge conjugated same flavor leptons can be removed very efficiently. The two like sign leptons are required to be isolated and having a transverse momentum above 15 GeV. In addition, missing transverse energy above 20 GeV is demanded to account for neutrinos. An integrated luminosity of 636 pb^{-1} has been used leading to an exclusion limit of 3.88 pb for a Higgs mass of 115 GeV.

4. $\mathbf{H \to WW^* \to \ell^+\ell^-\nu\bar{\nu}}$, $\ell = \mathbf{e}, \mu$

The Higgs invariant mass cannot be reconstructed in the case of leptonical W boson decay since the neutrinos leave the collision undetected. On the other hand one can exploit the spin correlation between the two leptons to discriminate background where two lepton candidates are not originating via a W boson from a scalar particle like the SM Higgs boson. The spins of the two W bosons originating from a scalar Higgs boson have to add up to zero. Due to the left-handed character of the electro-weak interaction the two leptons tend to be emitted collinear. To select the events two charge conjugated leptons are required. One of them has to have a transverse momentum above 20 GeV and the other above 10 GeV. Missing transverse energy has to exceed one forth of the Higgs mass for which a limit is being derived. The invariant di-lepton mass has to exceed 16 GeV and to be smaller than $M_H - 5$ GeV. An integrated luminosity of 360 pb^{-1} has been used. The difference in azimuthal angle between the two leptons is histogrammed and fitted to derive a limit. For a Higgs mass of 120 GeV the exclusion limit at 95% C.L. is 4.5 pb.

The DØ analysis uses an integrated luminosity of 950 pb^{-1}. For a Higgs mass of 120 GeV 31 events are observed and 32.7 ± 2.3 are predicted, leading to an exclusion limit of 6.3 pb at 95% C.L.

Exclusion limits normalized to the SM cross section of all discussed analyses versus Higgs mass are shown in Fig. 5 (left), [3].

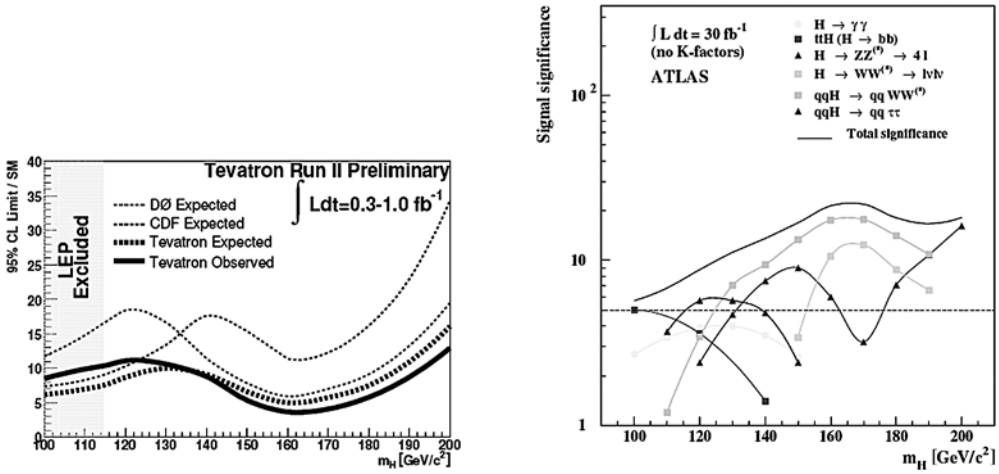

Fig. 5 – DØ and CDF Higgs exclusion limits normalized to the cross section predicted by the SM [3] (left). The significance for the SM Higgs boson discovery as a function of M_H from the ATLAS collaboration [9] (right).

3.1.2. Higgs searches at LHC

At the LHC, all production modes will play an important role, due to the higher statistics available. In particular, it is natural to distinguish between a light and a heavy mass region, as become evident by simultaneously looking at both production cross section, Fig. 4 (right) and decay branching ratios, Fig. 1 (left), over the entire 115–1000 GeV SM Higgs boson mass range. In the region of $M_H < 130$–140 GeV the SM Higgs boson at the LHC will be searched mainly in the following channels: $gg \to H$, $H \to \gamma\gamma$, W^+W^-, ZZ, $qq \to qqH$, $H \to \gamma\gamma$, W^+W^-, ZZ, $\tau^+\tau^-$, $q\bar{q}$, $gg \to t\bar{t}H$, $H \to b\bar{b}$, $\tau^+\tau^-$, while above that region, for instance for $M_H > 130$–140 GeV, the discovery modes will be: $gg \to H$, $H \to \gamma\gamma$, W^+W^-, ZZ, $qq \to qqH$, $H \to \gamma\gamma$, W^+W^-, ZZ, $q\bar{q}$, $gg \to t\bar{t}H$, $H \to W^+W^-$.

These modes have been used by both ATLAS and CMS to provide the discovery reach at LHC as illustrated in Fig. 5 (right). Other important channels in the low mass region are the inclusive Higgs production with $H \to \gamma\gamma$ and, below $M_H = 130$ GeV, $t\bar{t}H$ with $H \to b\bar{b}$. In the high mass region, the inclusive production with $H \to ZZ$, WW dominates.

3.2. PROSPECTS FOR MEASURING HIGGS PROPERTIES

If some Higgs-like particle is discovered, one of course wants to measure its properties: mass, width, spin, CP quantum numbers, coupling to fermions and gauge bosons, as well as self-couplings. The LHC will have the capacity of

measuring several of its properties at some level of accuracy. In particular, it will be able to measure its mass, width and coupling ratios. At the same time, the charge and color quantum numbers of the newly discovered particle will be established by detecting a single production channel. A precise determination of its spin and parity will probably require more statistics than available at the LHC and will have to wait for the ILC.

3.2.1. Measurements at LHC

1. Mass and width

The mass is extracted directly by measuring the position of the peak in the invariant mass distribution, for the following channels: $H \to \gamma\gamma$, $t\bar{t}$, $W(H \to b\bar{b})$, $H \to ZZ^{(*)} \to 4\ell$, as well as $H \to \tau\tau \to \ell$ + hadrons, where one of the τ leptons decays leptonically and the other hadronically. The mass can also be extracted indirectly, by comparing various distributions, which are sensitive to the Higgs mass, with Monte Carlo simulations. This can be done for the following channels: $H \to WW \to \ell\nu\ell\nu$, $W(H \to WW) \to (\ell\nu(\ell\nu\ell\nu))$ and $H \to \tau\tau \to \ell\ell$.

Using 300 fb^{-1} of data and combining the expected results of the CMS and ATLAS [10] experiments, a relative precision on M_H of 0.1 % can be obtained for M_H = 100–400 GeV. For $M_H > 400$ GeV, the precision degrades down to 1% at M_H = 700 GeV.

Regarding the Higgs width, a direct measurement is only possible for $M_H > 200$ GeV, when the Higgs width becomes comparable or larger than the intrinsic detector resolution. For instance, $\Gamma_H \sim 3$ MeV for $M_H = 110$ GeV and $\Gamma_H \sim 1$ GeV for M_H = 200 GeV. In this case, for a heavy Higgs boson a relative precision of 6% for the Higgs boson width can be reached.

2. Spin and CP eigenvalues

If a Higgs-like particle is observed, it is important to know if it has the relevant spin and CP eigenvalues, $J^{CP} = 0^{++}$. ATLAS [11] has studied the possibility to use angular distributions and correlations in the $H \to ZZ \to 4\ell$ channel for $M_H > 200$ GeV, in order to extract the J and CP state of the resonance. Two angular distributions are investigated: the polar angle of the leptons relative to the Z boson in the Higgs rest frame, cosθ and the angle between the decay planes of the two Z bosons in the Higgs rest frame. The measured distributions are compared to those of hypothetical particles with the following (J, PC) values: (0, 1) which is the SM scalar case, as well as (0, –1), (1, 1) and (1, –1), respectively the pseudoscalar, the vector and axial vector cases.

For 100 fb^{-1}, the polar angle distribution enables to exclude non-SM (J, CP) values for $M_H > 250$ GeV [11]. For 300 fb^{-1} and $M_H > 200$ GeV, (J, CP) = (1, 1) and (1, –1) can be ruled out with respectively 6.4σ and 3.9σ significances [11]. For

Higgs masses $M_H < 200$ GeV the azimuthal separation of leptons in the fusion channel followed by the $H \to WW \to \ell\nu\ell\nu$ decay can be exploited to extract significances on the spin and CP eigenvalues, but this is still work in progress.

3. Couplings

Many recent studies have pointed out that the LHC, under minimal theoretical assumptions, will have the potential to measure several Higgs boson couplings with an accuracy in the 10–30 % range. The proposed strategy [12] consists of measuring the production-decay channels for a light or heavy Higgs boson respectively, and combine them to extract individual partial widths or ratios of partial widths. If a given production-decay channel is observed, one can write that the experimentally measured product of production cross section times decay branching ratio corresponds, in the narrow width approximation, to the following expression:

$$(\sigma_{prod}(H)BR(H \to XX))^{exp} = \frac{\sigma^{th}_{prod}(H)}{\Gamma^{th}_{prod}} \frac{\Gamma_{prod}\Gamma_{decay}}{\Gamma},$$

where Γ_{prod} and Γ_{decay} are the partial widths associated with the production and decay channels respectively, while Γ is the Higgs total width. The coefficient $\sigma^{th}_{prod}(H)/\Gamma^{th}_{prod}$ can be calculated, while Γ_{prod}, Γ_{decay} and Γ is what needs to be determined. To each production-decay channel one can therefore associate a measurable observable $Z^{prod}_{decay} = \frac{\Gamma_{prod}\Gamma_{decay}}{\Gamma}$. Z^{prod}_{decay} is obtained from the experimental measurement of $(\sigma_{prod}(H)BR(H \to XX))^{exp}$, normalized by the theoretically calculable coefficient $\sigma^{th}_{prod}(H)/\Gamma^{th}_{prod}$. A signal in a certain production-decay channel will measure Z^{prod}_{decay}, and therefore the product of Higgs couplings $y^2_{prod}y^2_{decay}$, since $\Gamma_{prod} \simeq y^2_{prod}$ and $\Gamma_{decay} \simeq y^2_{decay}$. Combining many different production-decay channels, a system of equations is obtained. Ratios of partial widths Γ_i/Γ_j, and therefore ratios of Higgs couplings can be derived in a model independent way. Individual partial widths can be obtained with further assumptions: the total width is the sum of all SM partial widths, meaning that there is no new physics or invisible width contributions; the y_W and y_Z couplings are related by the $SU(2)_L$ weak isospin symmetry, required by the fact that, in $qq \to qqH$, the $W^+W^- \to H$ and $ZZ \to H$ fusion processes cannot be distinguished experimentally. The accuracy with which both individual couplings and ratios of couplings can be extracted is mainly determined by the experimental error on the Z^{prod}_{decay} measurements and by the theoretical uncertainty on the prediction of σ^{th}_{prod}.

Assuming 300 fb^{-1} and for $110 < M_H < 150$ GeV, the squared couplings can be extracted [13] with a relative precision of 25% to 60%, except for $g^2(H, b)$ where the relative error reaches from 80% to 300%, suffering from the fact that the $H \to b\bar{b}$ channel is difficult to detect. The total width can be estimated with a relative error of 50% to 75%. For $160 < M_H < 190$ GeV the squared coupling measurement profits from the high branching ratios of $H \to WW, ZZ$ and resolutions of 10% to 15% are attained. The same relative error is obtained for the total width measurement.

4. Self-coupling

To establish the Higgs mechanism experimentally, one must reconstruct the Higgs potential as a function of the physical Higgs boson:

$$V = (M_H^2/2)H^2 + (M_H^2/2v)H^3 + (M_H^2/8v^2)H^4.$$

A determination of the Higgs boson mass, which satisfies in the SM at the tree level the relation $M_H = \sqrt{2\lambda v}$, will provide an indirect information about the Higgs potential and its self-coupling λ. The measurement of the trilinear self-coupling $\lambda_{HHH} = \frac{6}{\sqrt{2}}\lambda v$ offers an independent determination of the shape of the Higgs potential. In case of disagreement, the comparison between these two measurements would give interesting hints about new physics.

The following channel can be used at the LHC: $gg \to HH \to (W^+W^-)(W^+W^-) \to (jetjet\ell^{\pm})(jetjet\ell^{\pm})$. The visible system invariant mass M_{vis} distribution is used to extract the value of $\lambda = M_H^2/2v$. Two extra samples with non-SM values of $\lambda_{HHH} = \lambda/\lambda_{SM}$ (0 and 2) are generated. The 95% C.L. bounds are derived from a χ^2 fit to M_{vis}. It is assumed that the SM is valid except for the self-coupling, that M_H is precisely known and that $BR\,(H \to WW)$ is known to 10% or better. Assuming 300 fb^{-1}, $\Delta\lambda_{HHH} = (\lambda - \lambda_{SM})/\lambda_{SM} = -1$ is excluded at 95% C.L. or better and λ can be determined with a relative error of –60% and +200%, respectively the lower and upper 1σ errors. With the same integrated luminosity, the significance for a SM signal is greater than 1σ for $150 < M_H < 200$ GeV and approximately 2.5σ for $160 < M_H < 180$ GeV [14].

3.2.2. Measurements at ILC

An e^+e^- collider provides a very clean environment, with relatively simple signatures and very good signal to background ratios for Higgs boson analyses. Therefore, one of the most important roles that a high energy e^+e^- collider as the ILC will play is to unambiguously identify any new particle discovered at the LHC,

through a complete program of precision measurements. We expect that the mass, width, spin and couplings of any Higgs boson candidates to be determined at the few percent level.

The most important SM Higgs boson production processes in e^+e^- collisions are illustrated in Figs. 6 and 7 and are: the Higgsstrahlung or associated production with Z gauge bosons, $e^+e^- \to ZH$; the vector boson fusion (W^+W^-, ZZ) production, $e^+e^- \to H\nu\overline{\nu}$ and $e^+e^- \to He^+e^-$ respectively; the associated production with a $t\overline{t}$ pair, $e^+e^- \to Ht\overline{t}$. The cross sections of these processes as function of the corresponding Higgs masses are illustrated in Fig. 8 for various center-of-mass energies, $\sqrt{s}$. The $e^+e^- \to ZH$ and $e^+e^- \to H\nu\overline{\nu}$ are the main production modes for a SM Higgs bosons. Their relative size varies with the center-of-mass energy, since $\sigma(e^+e^- \to ZH)$ scales as $1/s$ (s-channel process), while $\sigma(e^+e^- \to H\nu\overline{\nu})$ scales as log$s$ (t-channel process). $e^+e^- \to H\nu\overline{\nu}$ always dominates over $e^+e^- \to He^+e^-$ by

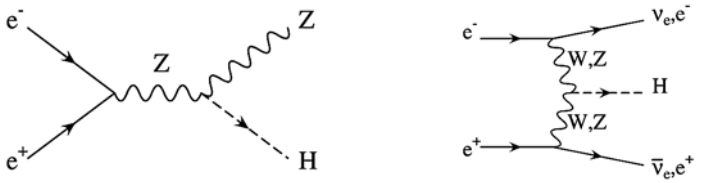

Fig. 6 – Higgs boson production via Higgsstrahlung and W^+W^-, ZZ fusion at e^+e^- colliders.

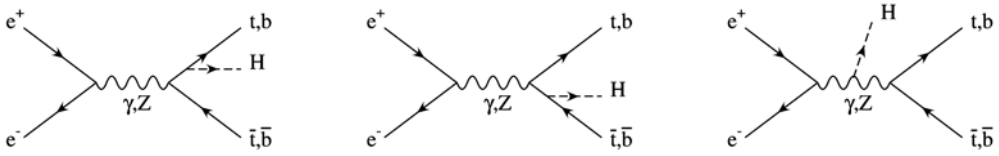

Fig. 7 – Higgs boson production in association with $t\overline{t}$ pairs at e^+e^- colliders.

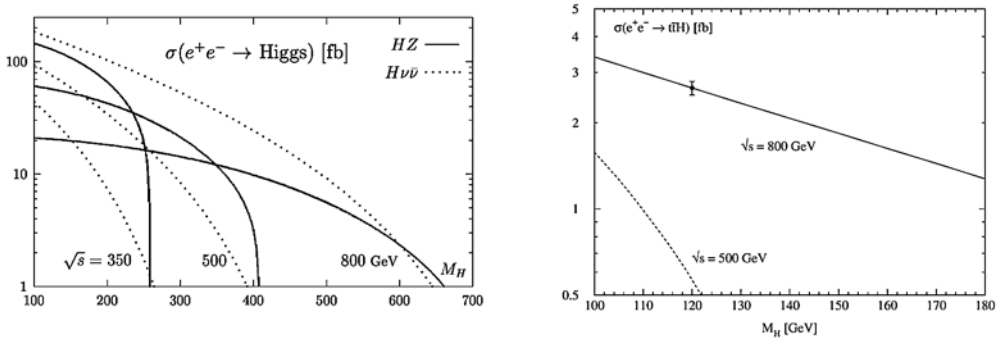

Fig. 8 – SM Higgs boson production cross sections in e^+e^- collisions, for various center-of-mass energies ($\sqrt{s}$). From Ref. [15].

almost one order of magnitude. The $t\bar{t}H$ production is always very rare, in particular at center-of-mass energies around 500 GeV or lower, but it plays a really important role at higher energies, around 800 GeV – 1 TeV, for the determination of the top-Yukawa coupling. Other rare production modes that play an important role in determining some Higgs boson properties are the double Higgs boson production modes: $e^+e^- \to HHZ$ and $e^+e^- \to HH\nu\bar{\nu}$.

With the ILC running at energies between 350 GeV and 1 TeV, one or more Higgs bosons can be observed over the entire mass spectrum and all its properties can be precisely studied. Reconstructing the recoiling $\ell^+\ell^-$ mass (for $\ell = e, \mu$) in $e^+e^- \to HZ \to H\ell^+\ell^-$, where the Z is mono-energetic, allows an excellent and model independent determination of the Higgs boson mass. $Z \to q\bar{q}$ decays can also be used and actually provide a very large data sample. Accuracies of the order of 50–80 MeV can be obtained, depending on the center-of-mass energy and the Higgs boson mass. The spin and parity of the Higgs boson candidate, expected to be $J^P = 0^+$, can be determined in several ways: from the onset of $\sigma(e^+e^- \to ZH)$, since the energy dependence near threshold strongly depend on the J^P quantum number of the radiated H, see Fig. 9; from the angular distribution of H and Z in $e^+e^- \to ZH \to 4f$; from the differential cross section in $e^+e^- \to Ht\bar{t}$.

Finally, a high energy ILC will measure the Higgs boson couplings to unprecedented precision and in a model independent way. Thanks to the precise knowledge of the initial state energy configuration, once the initial state radiation, or beamstrahlung, has been properly taken into account, one can measure both, $\sigma(e^+e^- \to HZ \to H\ell^+\ell^-)$ and $\sigma(e^+e^- \to W^*W^*\nu\bar{\nu} \to H\nu\bar{\nu})$, reconstructing the mass recoiling against the $\ell^+\ell^-$ or $\nu\bar{\nu}$ pair, and from there determine in a model independent way the isolated HZZ and HWW couplings. At a lepton collider the Higgs couplings to the weak gauge bosons, namely the Higgs coupling associated

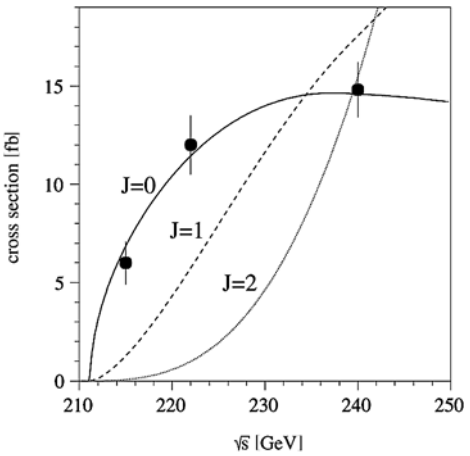

Fig. 9 – The $e^+e^- \to ZH$ cross section energy dependence near threshold for $M_H = 120$ GeV and spin $JP = 0^+, 1^-, 2^+$. From Ref. [16].

to the production mode, y_{prod}, can be isolated model independently. Any other coupling can then be also determined in a model independent way, measuring the individual $BR(H \to XX)$ in $e^+e^- \to HZ$ followed by $H \to XX$. Several recent studies have confirmed the possibility of determining Higgs couplings to both gauge boson and fermions within a few percent (2–5%). For instance, for a Higgs boson of $M_H = 120$ GeV, the bottom-Yukawa coupling, y_b, could be determined within 2%, the τ one, y_τ, within 5%, and the charm quark one, y_c, within 6% due to a larger error on the charm quark mass. This will test in a very stringent way the proportionality of the Higgs couplings to the mass of the interacting fermion. Even the indirect coupling of the Higgs boson to a pair of gluons, arising at the one-loop level, will be determined with a precision of 4–5%. This will allow an indirect check of the top-Yukawa coupling for a SM Higgs boson, when the top-quark loop dominates, or will result in some anomalous coupling if new physics contributes in the loop.

The only problem in completing a full study of the Higgs boson coupling is the determination of the top-quark Yukawa coupling, and of the Higgs self coupling. The top-quark Yukawa coupling is indirectly determined by measuring the $t\bar{t}H$ cross section, when the Z contribution is under control. The cross section is very small at $\sqrt{s} = 500$ GeV, and peaks around $\sqrt{s} = 800$ GeV. Recent studies show that with the ILC operating at $\sqrt{s} = 500$ GeV the top-Yukawa coupling, y_t, for $M_H = 120$ GeV Higgs boson, will probably be determined only at the 25% precision level, while with the ILC operating at $\sqrt{s} = 800$ GeV precision as high as 5–6% becomes available.

The production of Higgs boson pairs is very rare, however the results of preliminary analyses of the Higgs boson self-coupling [17, 18] are encouraging. The ILC could achieve about 20–30% measurement of λ over a broad mass range.

Finally, the total width of a SM-like Higgs boson can be determined in a model independent way by using any well measured branching ratio. For example, one can use that $\Gamma = \Gamma(H \to WW^*)/BR(H \to WW^*)$, where $BR(H \to WW^*)$ is measured directly and $\Gamma(H \to WW^*)$ can be calculated from the direct determination of the HWW coupling.

4. CONCLUSIONS

The LEP experiments established the current lower limit on the Higgs mass of 114.4 GeV at 95% C.L. The Tevatron experiments have searched for the SM Higgs bosons in a wide range of channels, using data corresponding to an integrated luminosity of 1 fb^{-1} in Run II. No deviation from the SM background expectation has been observed so far.

The LHC will be the machine that can discover a SM-like Higgs boson of any mass between 115 GeV and 1000 GeV, but also many of its properties can be investigated. The LHC can also make a step towards the difficult determination of the SM Higgs potential, at least the measurement of the Higgs triliniar self-coupling. The ILC will be able to make improvements to the LHC's measurements and determine precisely the nature of the Higgs sector.

Acknowledgments. The author would like to thank W. Lohmann from DESY – Zeuthen for carefully reading this manuscript. This work was supported by the CEEX Program of the Romanian Ministry of Education and Research, contracts 7613/12.10.2005 and M3 118/01.08.2006.

REFERENCES

1. F. Englert, R. Brout, Phys. Rev. Lett. **13**, 321 (1964);
   P. W. Higgs, Phys. Rev. Lett. **13**, 508 (1964);
   G. S. Guralnik, C. R. Hagen, T. W. B. Kibble, Phys. Rev. Lett. **13**, 585 (1964).
2. M. E. Peskin, D. V. Schroeder, *An Introduction to Quantum Field Theory*, Harpen Collins Publisher, (1995).
3. A. Djouadi, J. Kalinowski, M. Spira, Comp. Phys. Comm. **108**, 56 (1998), hep-ph/9704448.
4. A. Djouadi, *The anatomy of electro-weak symmetry breaking I: The Higgs boson in the standard model*, hep-ph/0503172.
5. ALEPH, DELPHI, L3 and OPAL Coll., Phys. Lett. **B565**, 61 (2003).
6. Tevatron-for-LHC Report: Higgs, hep-ph/0612172.
7. http://www-cdf.fnal.gov/physics/exotic/exotic.html,
   http://www-d0.fnal.gov/Run2Physics/WWW/results/higgs.htm
8. DØ and CDF Coll., CDF Note 8384 and DØ Note 5227.
9. ATLAS Coll., Eur. Phys. J. **C32S2**, 19 (2004).
10. ATLAS Coll., Atlas Physics TDR, CERN/LHCC/99-14 and CERN/LHCC/99-15.
11. C. P. Buszello, I. Fleck,P. Marquard, J. J. van der Bij, Eur. Phys. J. **C32**, 209 (2004).
12. D. Zeppenfeld, R. Kinnunen, A. Nikitenko, E. Richter-Was, Phys. Rev. **D62**, 013009 (2000).
13. M. Duehrssen, ATL-PHYS-2003-030, M. Duehrssen, S. Heinemeyer, H. Logan, D. Rainwater, G. Weiglei, D. Zeppenfeld, Phys. Rev. **D70**, 113009 (2004).
14. U. Baur, T. Plehn, D. Rainwater and D. Zeppenfeld, Phys. Rev. **D67**, 033003 (2003).
15. J. A. Aguilar-Saavedra *et al.*, hep-ph/0106315.
16. M. T. Dova, P. Garcia-Abia, W. Lohmann, hep-ph/0302113.
17. C. Castanier, P. Gay, P. Lutz, J. Orloff, LC-PMSM-2000-061.
18. K. Mönig, A. Rosca, submitted to Pramana J. Phys.